Location of Series-Connected Controllers to Reduce Proximity to Transient Instability based on a Trajectory Sensitivities Approach

Enrique A. Zamora-Cárdenas, Claudio R. Fuerte-Esquivel, *Senior Member IEEE*

***Abstract*—Determining suitable locations of series-connected controllers is a practical problem when it is necessary to install them in modern power systems. The aim of this paper is to find the best location of series controllers in order to reduce the proximity to instability of a current operating point of a power system, from a transient stability viewpoint. In order to achieve this goal, a general approach has been developed based on an index of proximity to instability and trajectory sensitivity analysis. An efficient way to carry out multi-parameter sensitivities is formulated analytically and solved simultaneously with the set of differential-algebraic equations representing power systems dynamics within a single-frame of reference. Simulations are performed on 9-bus and 39-bus benchmark power systems for illustration purposes. Results show that the proposed approach provides the most effective location of series-connected controllers to improve the power systems transient behavior.**

***Index Terms*—Transient stability, trajectory sensitivities, sensitivity index, series compensation.**

I. Introduction

Advances in Flexible AC Transmission Systems (FACTS) controllers have led to their application in improving electric power systems' controllability [1],[2]. It has been recognized that the location of these controllers has a large impact on their performance with regard to the control objective to be fulfilled. The best allocation for one objective may be less suitable for another objective. This has motivated the development of several kinds of approaches for finding proper locations of FACTS controllers in order to improve the power system's static or dynamic performance. Methodologies based on singular value decomposition [3], bus participation factor [4], augmented Lagrange multipliers [5], heuristic methods [6], [7], mixed integer linear programming [8] and sensitivity-based approach [9], [10] have been proposed to allocate controllers to satisfy suitable steady-state control objectives. On the other hand, proper locations to improve damping of low frequency electromechanical oscillations have been determined based on modal analysis [11], [12], [13] and residue method [14], [15].

Transient stability analysis is also an essential study in the operation and planning of electric power system [16]. If this study determines that a rotor angle transient instability takes place due to large electromechanical oscillations among generation units and lack of synchronizing torque on the system, control actions have to be taken to prevent partial or complete service interruption. Among different preventive control measures, it is possible to apply series compensation in a proper place to regain an acceptable state of equilibrium after the disturbance by improving the system's stability condition [16]. The stability condition can be computed by a time domain simulation which is applicable for arbitrarily complicated models, and it is feasible for large-scale power system analysis. However, this simulation only provides information about a single scenario, and repeated simulations have to be done to assess a degree of system's stability or instability.

Trajectory sensitivity (TS) analysis overcomes the need of repetitive simulation. In this approach, a linearization is carried out around a nominal trajectory rather than around an equilibrium point, such that it is possible to assess variations in the nominal transient trajectory resulting from small perturbations in the underlying parameters and/or initial conditions [17]. These results are only valid for the equilibrium point that defines the nominal trajectory. Applications of TS includes the study of parameter uncertainty in system behaviour [18],[19], determination of well-conditioned parameters for reliable estimation [20],[21],[22], and determination of critical machines which are likely to go unstable for a given loading conditions and a specified contingency [23], among others [24].

Owing to the fact that TS analysis provides a qualitative measure of how stable or instable a particular case may be, and valuable insights into the influence of parameters on the nominal transient trajectory of the system, this approach was applied to successfully analyze the Nordel power grid disturbance on January 1, 1997 [25]. Sensitivities of relative rotor angle with respect to line impedances were used to identify which line was most sensitive with respect to system stability and to indicate the effect of this line with respect to different generators in the system. Based on these results, authors suggested that the TS approach could be used to

This work was supported by CONACyT, Mexico under the scholarship 169415.

A. Zamora-Cárdenas and Claudio R. Fuerte-Esquivel are with the Electrical Engineering Faculty, Universidad Michoacana de San Nicolás de Hidalgo (UMSNH), Morelia, Michoacan, 58000, Mexico (email:reycoliman2002@hotmail.com, cfuerte@umich.mx). The first author is also with the Instituto Tecnologico Superior de Irapuato (ITESI), Gto., Mexico.

978-1-4244-6551-4/10/$26.00 ©2010 IEEE

choose effective locations of FACTS devices. This idea is revisited and applied in this paper to determine the suitable locations of series compensators.

Since the improvement of transient stability can be considered as a problem of controlling transient trajectories by a change in parameters, TS can be used to judge the effectiveness of FACTS controllers in improving stability. This study was performed in [26] considering static models of a thyristor controlled series compensator (TCSC) and a static synchronous compensator (STATCOM). The effects of these compensators were assessed by placing them individually at each transmission line, one at the time, and calculating a post-fault stability condition based on the numerical formulation of the trajectory sensitivity. In this case, sensitivities of state trajectories with respect to system parameters are found by perturbing the selected parameter from its nominal value, and making the division of the changes in the state variables over the parameter perturbation; i.e. $\Delta x / \Delta\beta$, at each time step of integration. This approach requires two time domain simulations for each sensitivity, and the selection of the size of the parameter perturbation. The later is selected heuristically such that the numerical sensitivity be very close to the analytically calculated trajectory sensitivity value.

The most effective location of a series compensation can be obtained by the approach suggested in [26] for a given one fault scenario after the computation of Γ time domain simulations, where Γ=(1+number of parameters (*Np*)). As the number of fault scenarios increases by *nf* times, the required number of time domain simulations to assess the parameters' effects is actualized by $\Gamma = nf^{*}\Gamma$.

A radical approach is applied in this paper to avoid the problem of performing a great number of time domain simulations to determine the most effective location of a series compensation. This consists of formulating the trajectory sensitivities analytically, such that only one time domain simulation is required to assess the effect of one parameter for a given fault scenario. The extension to multi-parameter sensitivities computations is straightforward. The number of simulations only increases directly proportional to the number of fault scenarios and is not a function of the *Np* parameters considered at each fault study.

The remaining of the paper is organized as follows. Section II provides the mathematical models of the electric power components considered in the studies. Section III presents the detailed analytical formulation to carry out multi-parameter trajectory sensitivity studies, while Section IV describes the application of this formulation to select the most effective location of a series compensation. In Section V, two case studies based on the WSCC 9-buses 3-generators system, and on the New England 39-buses 10-generators system, are analyzed and discussed in detail. Lastly, Section VI points out the conclusions.

II. Power Systems Models

An electric power system can be represented analytically by a set of parameter dependent differential equations constrained by a set of algebraic equations (DAEs), as given by (1), where x is a vector of the dynamic state variables, y is a vector of the algebraic variables (usually complex node voltages), and β is a set of non-time varying system parameters

$$\begin{aligned} &\dot{x} = f(x, y, \beta) && f : \Re^{n+m+p} \rightarrow \Re^{n} \\ &0 = g(x, y, \beta) && g : \Re^{n+m+p} \rightarrow \Re^{m} \\ &x \in X \subset \Re^{n} \quad y \in Y \subset \Re^{m} && \beta \in \boldsymbol{\beta} \subset \Re^{p} \end{aligned} \qquad (1).$$

Due to the fact that transmission network dynamics are much faster than dynamics of the equipment or loads, it is considered that the variables y change instantaneously with variations of the x states. Hence, only the dynamics of the equipment, e.g. generators, controls, FACTS devices, and load at buses, are explicitly modeled by the set of differential equations (1). The set of algebraic equations express the mismatch power flow equations at each node. As the power system can be viewed as an interconnection of several electric power plant components, particulars of each model considered in this paper are given below. All variables are given in per unit, unless otherwise specified.

A. Generator

In this paper, the two-axis generator model is considered with a field and a damper winding on the *d*-axis as well as a damper winding on the *q*-axis.

1) Rotor equations

The rotor mechanical model is given by the swing equations. For the i^{th} generator, these equations are

$$\begin{aligned} &\dot{\delta}_i = \omega_i - \omega_0 \\ &\dot{\omega}_i = \frac{\omega_0}{2H_i}\left(P_{Mi} - P_{ei} - D_i\left(\omega_i - \omega_0\right)\right) \\ &P_{ei} = E_{qi}^{'} I_{qi} + E_{di}^{'} I_{di} + (X_{qi}^{'} - X_{di}^{'}) I_{di} I_{qi} \end{aligned} \qquad (2)$$

where $2H_i$ is the moment of inertia in seconds (sec), D_i is the damping constant, P_{ei} is the generator's electrical power associated with the internal voltage source, P_{Mi} is the turbine mechanical power injection, δ_i is the generator's rotor angle in radians (rad), ω_0 is the synchronous speed in rad/sec, and ω_i is the actual rotor speed in rad/sec.

The equations of the two electrical systems on the rotor are

$$\begin{aligned} &\dot{E}_{qi}^{'} = \frac{-E_{qi}^{'} - (X_{di} - X_{di}^{'}) I_{di} + E_{fdi}}{T_{d0i}^{'}} \\ &\dot{E}_{di}^{'} = \frac{-E_{di}^{'} + (X_{qi} - X_{qi}^{'}) I_{qi}}{T_{q0i}^{'}} \end{aligned} \qquad (3)$$

where $E_{di}^{'}$ and $E_{qi}^{'}$ are the transient internal voltage magnitudes on d and q axes, respectively, I_{di} and I_{qi} are the stator currents on d and q axes, X_{ki} and $X_{ki}^{'}$ are the synchronous steady state and transient state reactances on axes k=q, and k=d, respectively, $T_{d0i}^{'}$ and $T_{q0i}^{'}$ are the constant time on d and q axes, respectively, lastly, E_{fdi} is the *DC* controlled voltage field.

2) Stator equations

The algebraic equations (4) can be obtained by neglecting both stator transients and stator resistance, where V_i and θ_i are the magnitude and phase angle voltages at generator terminals on the network side, and the generated power is measured at terminals,

$$\begin{aligned}
E'_{qi} &= V_i \cos(\delta_i - \theta_i) + X'_{di} I_{di} \\
E'_{di} &= V_i \sin(\delta_i - \theta_i) - X'_{qi} I_{qi} \\
P_{gei} &= I_{di} V_i \sin(\delta_i - \theta_i) + I_{qi} V_i \cos(\delta_i - \theta_i) \\
Q_{gei} &= I_{di} V_i \cos(\delta_i - \theta_i) - I_{qi} V_i \sin(\delta_i - \theta_i)
\end{aligned} \qquad (4).$$

B. Excitation system

The excitation system is considered as shown in Fig. 1, which includes max/min ceiling limits, with its equation given by (5)

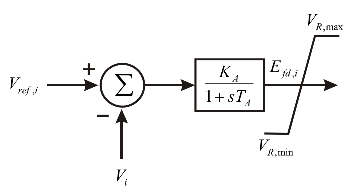

Fig.1. Excitation system.

$$\dot{E}_{fdi} = \frac{K_{Ai}(V_{refi} - V_{ti}) - E_{fdi}}{T_{Ai}} \qquad (5)$$

where E_{fdi} is the DC controlled voltage field, V_{refi} is the reference node voltage, V_{ti} refers to the voltage at the generator terminal, K_{Ai} is the control gain and T_{Ai} is the excitation system time constant.

C. Load

The classical constant impedance load model is considered to capture the transient system trajectories. The impedance values are computed at the *ith* system node from the stable equilibrium point that define the pre-disturbance operative state as follows:

$$P_{Li} = P^0_{Li}\left(\frac{V_i}{V_i^0}\right)^2; \quad Q_{Li} = Q^0_{Li}\left(\frac{V_i}{V_i^0}\right)^2 \qquad (6)$$

where P^0_{Li} and Q^0_{Li} are nominal demanded load and V_i^0 is the nominal voltage measured at the pre-disturbance state.

D. Network

This model consists of those equations expressing the active and reactive power balances at every system nodes. For the transmission element connected between nodes i and j, the active and reactive powers at the *ith* node are

$$\begin{aligned}
P_{ij} &= V_i^2 G_{ii} + V_i V_j (G_{ij} \cos(\theta_i - \theta_j) + B_{ij} sin(\theta_i - \theta_j)) \\
Q_{ij} &= -V_i^2 B_{ii} + V_i V_j (G_{ij} sin(\theta_i - \theta_j) - B_{ij} \cos(\theta_i - \theta_j))
\end{aligned} \qquad (7).$$

Assuming n_g generator nodes and n_{PQ} network nodes, V_k and θ_k are the magnitude and phase angle voltages at network nodes, $i = 1,\dots,n_g + n_{PQ}$, respectively, and $\vec{Y}_{ij} = G_{ij} + jB_{ij}$ is the admittance of the transmission element connected between nodes *i* and *j*.

The mismatch power equations at the network nodes are,

$$\begin{aligned}
P_{gei} &= P_{Li} + \sum_{j\in\Omega_i} P_{ij} && \forall i = 1,\dots,n_g \\
Q_{gei} &= Q_{Li} + \sum_{j\in\Omega_i} Q_{ij} && \forall i = 1,\dots,n_g \\
0 &= P_{Li} + \sum_{j\in\Omega_i} P_{ij} && \forall i = 1+n_g,\dots,n_{PQ} \\
0 &= Q_{Li} + \sum_{j\in\Omega_i} Q_{ij} && \forall i = 1+n_g,\dots,n_{PQ}
\end{aligned} \qquad (8)$$

where $\Omega_i = \{j : j \neq i\}$ is the set of nodes adjacent to *i*, and P_{Li} (Q_{Li}) is the active (reactive) power demanded by the load embedded at the *ith* node.

III. Trajectory Sensitivity Analysis

The constrained nonlinear dynamics of the power system are calculated by solving (1). State trajectories associated to this dynamic behavior will vary with small changes in the system parameters or the variables' initial conditions, and these variations can be quantified through a time domain sensitivity analysis. Nevertheless, there are two limitations in this approach, which relies on repeated simulations: (1) the computational burden required to calculate sensitivities, and (2) there is not a quantitative measure of the proximity to instability of the power system.

It has been demonstrated that it is possible to find out in a rigorous approach how sensitive the trajectories of each state are to changes in system parameters or initial conditions. The theoretical treatment to obtain analytical equations of trajectory sensitivities has been reported for both ODEs [27], [28] and DAEs [27], [29]. The analytical system sensitivities of (1) w.r.t. system parameters can be found for the post-disturbance state by perturbing β from its nominal value β_0, and considering that $f(x,y,\beta)$ and $g(x,y,\beta)$ have continuous first partial derivatives w.r.t. *x*, *y* and β from the disturbance clearing time t_{cl} to the end of the study time t_{end}, for all $(x,y,\beta) \in [t_{cl}, t_{end}] \mathrm{x} \Re^{nxmxp}$ and initial conditions $x(t_{cl}) = x_{cl}$, $y(t_{cl}) = y_{cl}$.

A. Analytical Formulation

Let β_0 be the nominal values of β, and assume that the nominal set of DAEs $\dot{x} = f(x,y,\beta_0)$, $0 = g(x,y,\beta_0)$ has a unique nominal trajectory solution $x(t,x_{cl},y_{cl},\beta_0)$ and $y(t,x_{cl},y_{cl},\beta_0)$ over $t \in [t_{cl}, t_{end}]$. Then, for all β sufficiently close to β_0, the set of DAEs (1) has a unique perturbed trajectory solution $x(t,x_{cl},y_{cl},\beta)$ and $y(t,x_{cl},y_{cl},\beta)$ over $t \in [t_{cl}, t_{end}]$ that is close to the nominal trajectory solution. This perturbed solution is given by

$$x(\cdot) = x_{cl} + \int_{t_{cl}}^{t_{end}} f\left(x(\cdot), y(\cdot), \beta\right) ds \\ 0 = g\left(x(\cdot), y(\cdot), \beta\right) \quad (9).$$

The sensitivities of dynamic and algebraic state vectors w.r.t. a chosen system parameter, $x_\beta = \partial x(\cdot)/\partial\beta$ and $y_\beta = \partial y(\cdot)/\partial\beta$, at a time t along the trajectory are obtained from the partial derivative of (9) w.r.t. β, i.e.

$$\frac{\partial x(\cdot)}{\partial\beta} = \int_{t_{cl}}^{t_{end}} \left(\frac{\partial f(\cdot)}{\partial x}\frac{\partial x}{\partial\beta} + \frac{\partial f(\cdot)}{\partial y}\frac{\partial y}{\partial\beta} + \frac{\partial f(\cdot)}{\partial\beta} \right) ds \\ 0 = \frac{\partial g(\cdot)}{\partial x}\frac{\partial x}{\partial\beta} + \frac{\partial g(\cdot)}{\partial y}\frac{\partial y}{\partial\beta} + \frac{\partial g(\cdot)}{\partial\beta} \quad (10).$$

Lastly, the smooth evolution of the sensitivities along the trajectory is obtained by differentiating (10) w.r.t. t, i.e.

$$\dot{x}_\beta = \frac{\partial f(\cdot)}{\partial x} x_\beta + \frac{\partial f(\cdot)}{\partial y} y_\beta + \frac{\partial f(\cdot)}{\partial\beta} \quad ; \quad x_\beta(t_{cl}) = 0 \\ \equiv f_x x_\beta + f_y y_\beta + f_\beta \quad (11)$$

and

$$0 = \frac{\partial g(\cdot)}{\partial x} x_\beta + \frac{\partial g(\cdot)}{\partial y} y_\beta + \frac{\partial g(\cdot)}{\partial\beta} \quad ; \quad y_\beta(t_{cl}) = 0 \\ \equiv g_x x_\beta + g_y y_\beta + g_\beta \quad (12)$$

where f_x, f_y, f_β, g_x, g_y and g_β, are time-varying matrices computed along the system trajectories.

B. Numerical solution

Trajectory sensitivities are computed by solving (11) and (12) simultaneously with (1) by using any numerical method. The staggered direct method (SDM) has been selected to solve sequentially the set of DAEs representing the power system and trajectory sensitivities [30]. The trapezoidal rule is applied to algebraize the differential equations, such that sets of DAEs (1), (11), and (12) are expressed by the following set of algebraic difference equations

$$F_1(\cdot) = x^{k+1} - x^k - \frac{h}{2}\left(f^{k+1} + f^k\right) = 0 \quad (13)$$

$$F_2(\cdot) = g^{k+1} = 0 \quad (14)$$

$$F_3(\cdot) = x_\beta^{k+1} - x_\beta^k - \frac{h}{2}\begin{pmatrix} f_x^{k+1}x_\beta^{k+1} + f_y^{k+1}y_\beta^{k+1} + f_\beta^{k+1} \\ + f_x^k x_\beta^k + f_y^k y_\beta^k + f_\beta^k \end{pmatrix} = 0 \quad (15)$$

$$F_4(\cdot) = g_x^{k+1}x_\beta^{k+1} + g_y^{k+1}y_\beta^{k+1} + g_\beta^{k+1} = 0 \quad (16)$$

where h is the integration time step, and the superscript k is an index for the time instant t_k at which variables and functions are evaluated, e.g. $x^k = x(t_k)$ and $f^k = f(x^k, y^k)$. Nonlinear equations (13) and (14) are coupled to the DAEs (1) whereas (15) and (16) correspond to the set of linear time variant DAEs (11) and (12).

The Newton-Raphson (NR) algorithm provides an approximate solution to (13) and (14) by solving for $\begin{bmatrix}\Delta x^k & \Delta y^k\end{bmatrix}^T$ in the linear problem $J^i \Delta X^i = -F(X^i)$, given in expanded form by (17), where J is known as the Jacobian matrix

$$\underbrace{\begin{bmatrix} I - \frac{h}{2}f_x^{k+1} & -\frac{h}{2}f_y^{k+1} \\ g_x^{k+1} & g_y^{k+1} \end{bmatrix}^i}_{J^i} \underbrace{\begin{bmatrix} \Delta x^k \\ \Delta y^k \end{bmatrix}^i}_{\Delta\chi^i} = -\underbrace{\begin{bmatrix} F_1(\cdot) \\ F_2(\cdot) \end{bmatrix}^i}_{F(\cdot)^i} \quad (17).$$

For given values $\begin{bmatrix}x^k & y^k\end{bmatrix}^T$, the method starts from an initial guess $\begin{bmatrix}x_0^{k+1} = x^k & y_0^{k+1} = y^k\end{bmatrix}^T$ and updates the solution at each iteration i, i.e. $\begin{bmatrix}x^{k+1} = x^k + \Delta x^k & y^{k+1} = y^k + \Delta y^k\end{bmatrix}^T$, until a convergence criterion is satisfied. The computational burden is directly associated to the size of the power system under study.

Once the states have been computed for a new time step, the sensitivity trajectories are calculated from the set of linear equations (18), which is derived from (15) and (16)

$$\underbrace{\begin{bmatrix} I - \frac{h}{2}f_x^{k+1} & -\frac{h}{2}f_y^{k+1} \\ g_x^{k+1} & g_y^{k+1} \end{bmatrix}}_{J} \underbrace{\begin{bmatrix} x_\beta^{k+1} \\ y_\beta^{k+1} \end{bmatrix}}_{S} = \underbrace{\begin{bmatrix} x_\beta^k + \frac{h}{2}\left(f_x^k x_\beta^k + f_y^k y_\beta^k + f_\beta^k + f_\beta^{k+1}\right) \\ -g_\beta^{k+1} \end{bmatrix}}_{\mathrm{B}} \quad (18).$$

The coefficient matrix on the left-side of (18) corresponds to the Jacobian matrix used in the final NR iteration to solve for x^{k+1} and y^{k+1} at (17). Based on this observation, the computational burden for the calculation of trajectory sensitivities is substantially reduced because the coefficient matrix is already factored, and only a forward/backward substitution is required for the solution of x_β^{k+1} and y_β^{k+1} at each discrete time t^{k+1} of the integration period [29].

The solution approach described above can be extended to compute the trajectory sensitivities associated to Np parameters of the system at each discrete time. In this case (18) is expressed as (19), which is solved Np times for the solution of $x_{\beta i}^{k+1}$ and $y_{\beta i}^{k+1}$ $\forall i = 1, \ldots, Np$, one at a time at the same time step

$$J\underbrace{\begin{bmatrix} S_{\beta 1} & S_{\beta 2} & \cdots & S_{\beta Np} \end{bmatrix}}_{S} = \underbrace{\begin{bmatrix} B_{\beta 1} & B_{\beta 2} & \cdots & B_{\beta Np} \end{bmatrix}}_{\mathrm{B}} \quad (19).$$

IV. Location of Series Compensation

Based on the observation that the more stressed the system is the larger its trajectory sensitivities are [17], it is possible to associate sensitivity information with the stability level of the system for a particular system parameter. The line susceptance's effect on the system's stability is measured by computing sensitivities of rotor angles trajectories w.r.t. transmission line susceptances, and measuring the proximity to instability.

An index of proximity to instability is determined based on the sensitivity norm obtained for the period $t \in [t_{cl}, t_{end}]$ for a n_g-machines system given by [23],

$$S_{Ni}(t)=\sqrt{\sum_{k=1}^{n_g}\left(\left(\frac{\partial\delta_k(t)}{\partial\beta_i}-\frac{\partial\delta_j(t)}{\partial\beta_i}\right)^2+\left(\frac{\partial\omega_k(t)}{\partial\beta_i}\right)^2\right)}\quad\forall i=1,\cdots,Np \tag{20}$$

where j denotes the reference machine.

The growth in the peak values of trajectory sensitivities indicates an underlying stability problem, and ideally $S_{Ni}(t)$ should be infinite at the point of the system's instability. Bearing this in mind, the index to proximity to instability is defined as the inverse of $S_{Ni}(t)$, $\eta_i = 1/\max\left|S_{Ni}(t)\right|$, which will approach zero as the systems moves toward instability [23]. Based on this result, the most effective location of series compensation corresponds to a transmission line whose small perturbations in its susceptance produce the lowest value of η_i.

V. Study Cases

The WSCC 9 buses, 3 generators and New England 39 buses, 10 generators systems shown in Figs 2 and 3, respectively, were analyzed to assess the effectiveness of the proposed approach. For the purpose of the studies presented in this paper, the two-axis generator model is considered which includes a simple faster exciter loop containing max/min ceiling limits, a field winding on *d*-axis and a damping winding on both *d*-axis and *q*-axis. The constant impedance load model is considered in accordance to the model used by commercial grade programs to undertake studies of transient stability. Lastly, transmission network components are represented by their steady-state models, because the network variables change instantaneously with variations of the dynamic variables.

The goal of the application is to determine the most appropriate line to be compensated to improve the transient stability for a set of possible faults taking place in a specified system's geographic area. This improvement is quantified through the sensitivity index given in Section IV considering the sensitivities w.r.t. the series susceptance of transmission lines. The disturbance consisted of a self-cleared three phase to ground fault at one end of the transmission element.

A. WSCC 9-buses, 3-generators system

For this system, faults are applied at each system's node, except at generator terminals, one at the time, and sensitivity indexes are computed for all transmission lines in order to determine which is the most suitable to be compensated. A stressed scenario was obtained for the *kth* fault by considering a clearing time (*cl*) value of 90% of the critical clearing time (*CCT*), $t_{cl}^k = 0.9t_{cct}^k$. The results obtained by the proposed approach are reported in Table I. It must be pointed out that 6 simulations were only required to obtain all results, whilst 42 simulations would be required if the numerical TS method was used.

From these results, it is observed that the stability index is most affected by changes in susceptances of lines connected between nodes 7-5 and 9-6, B_{7-5} and B_{9-6}. Hence, the best improvement of the system's transient behavior will be achieved by compensating the most sensitive line, which is connected between nodes 7-5. It must be pointed out that this line resulted in the best option for applying compensation for all cases. Therefore, a global stability control is accomplished by compensating this line.

Trajectory sensitivity analysis only indicates which line has to be compensated, but it does not indicate the type and degree of its compensation. However, this problem has been solved by a simple comparison of the system transient behavior without and with a specified level of compensation.

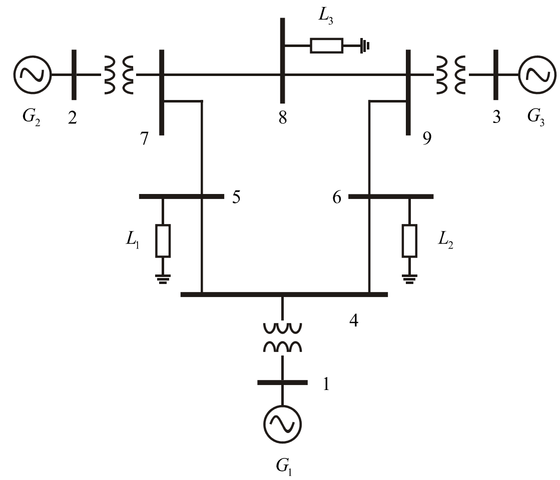

Fig. 2. WSCC 9-buses, 3-generators.

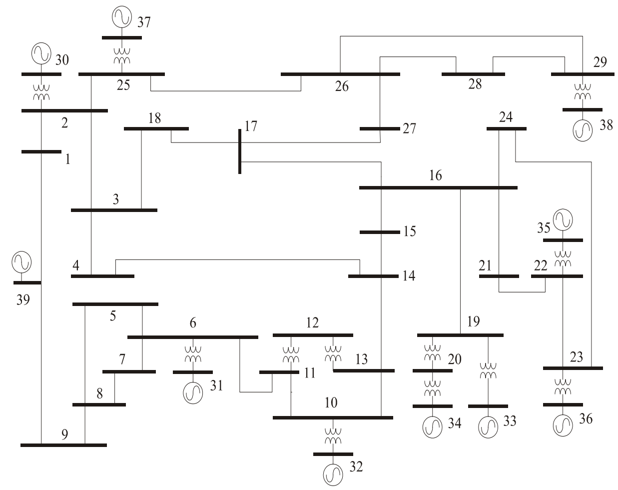

Fig. 3. New England 39-buses, 10-generators system.

TABLE I. η FOR EACH FAULT OF THE WSCC SYSTEM.

Line susceptance	η for a faulted node					
	7	8	9	6	5	4
B_{7-8}	5.99	8.51	7.25	10.3	7.85	9.82
B_{8-9}	4.84	6.77	4.18	6.46	6.09	6.93
B_{7-5}	0.74	0.77	1.07	0.86	0.82	0.85
B_{9-6}	1.32	1.26	1.59	1.35	1.35	1.39
B_{5-4}	3.33	3.49	4.84	3.81	3.57	3.77
B_{6-4}	7.66	7.31	7.70	7.68	7.77	7.82

Figure 4 shows three trajectories of the relative machine angle $\delta_2 - \delta_1$ considering no compensation, as well as 30 % of inductive and capacitive compensation of line 7-5. A fault was located at bus 6 and cleared at t_{cl}=0.339 sec. From this figure it is clear that a capacitive compensation improves the transient stability by damping the first oscillation, whereas an inductive compensation has the opposite effect.

Validation of the correct performance of the stability index is carried out by repeating the stability study stated above with a series capacitive compensation on the two lines with greater effect on the transient performance, i.e. lines 7-5 and 9-6, one at the time. The stability indexes for the base case indicated in Table I are $\eta(B_{7-5}) = 0.86$ and $\eta(B_{9-6}) = 1.35$, respectively. Fig. 5 shows the transient trajectories for all cases, confirming that the compensation on the most critical line 7-5 improved the first oscillation, better than line 9-6.

Lastly, a comparison of the *CCT*s for the base case and compensation on the line 7-5 case is shown in Table II regarding all faulted nodes, one at the time. It is observed in the last column of this table that in all cases the *CCT* improved when compensation is embedded in the transmission line, improving the transient stability margin.

B. New England 39-buses, 10-generators system

For the 39 buses 10 generators power system, the trajectory sensitivities have been used to increasing the transient stability margin in all nodes around a weak area in the power system. This area corresponds to the locations of faults with the lower critical clearing times computed by a contingency screening analysis on all non-generator nodes. For this network, the set of critical faulted nodes is given by 25 to 29. A fault in one of these nodes makes the generator embedded in the bus 38 lose synchronism with respect to the rest of generators, which in turn steers the system relatively faster to the instability than the remainder faulted nodes out of the mentioned area. As an example, Fig. 6 shows graphically how the generator at node 38 moves the rest of the machines forward for a fault applied at node 29.

The most effective location of series compensation is assessed by applying a fault at all nodes, except those with power injections, one at the time, and computing sensitivity indexes w.r.t. all line susceptances. Similarly to the study described in § V-*A*, the clearing time values were considered as 90% of the *CCT*s and the faults were self-cleared. In this case, the study required 29 simulations to identify the most influential line susceptance in the power system. It must be pointed out that if the same study was performed based on computing the trajectory sensitivities by using perturbed trajectories [26], 1015 time domain simulations would be required, significantly increasing the computational burden.

Table III reports the stability indexes resulting from the trajectory sensitivity analysis. Only lines with the lower values of stability indexes are reported. It is interesting to observe that these indexes correspond to faults applied at buses making up the weak area, which indicates that once the weak area has been identified, or an area of interest has been determined, it is only necessary to carry out the study in the set of nodes that comprise this area. The study in a sub-region of power system reduces substantially the computational burden (number of operations as well as memory requirements) especially for cases of large-scale systems.

Based on the results of Table III, the most effective location of series compensation is at the line with the most sensitive susceptance: the line connected between buses 26 and 29. This compensation will increase the "distance" of the system's trajectories to the stability boundary. This statement is confirmed by results shown in Fig. 7 which shows the relative rotor angle trajectory of the generator connected at node 38 w.r.t. the swing generator 39, δ_{38-39} for cases of non compensation, and 30% of capacitive compensation at the lines B_{26-29}, B_{26-28} and B_{25-26}, each one at the time. The fault was applied at bus 29 and cleared at its non compensation *CCT* given by $t_{cct} = 0.197$ sec. As was expected, all cases with series compensation improved the transient stability behavior, being the most effective when compensation is applied in line 26-29.

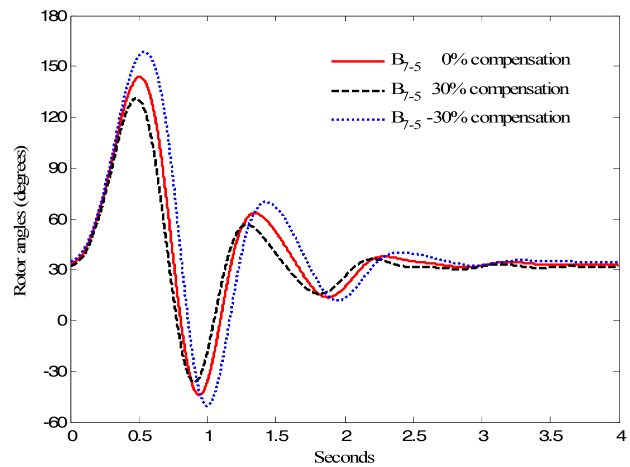

Fig. 4. δ_{2-1} with B_{7-5} compensated.

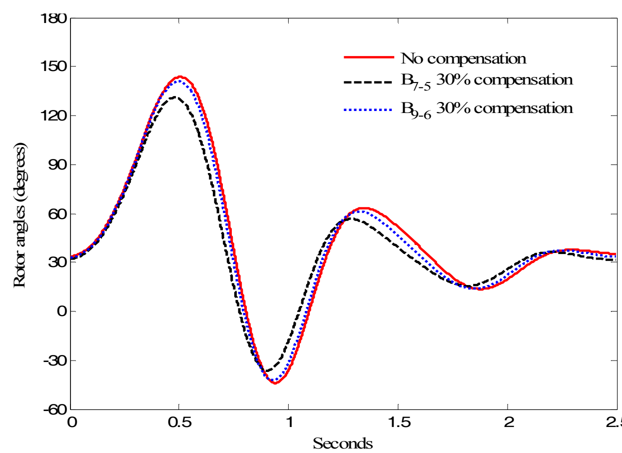

Fig. 5 Effect of lines compensation in the first oscillation.

TABLE II. *CCT*S WITH 30% COMPENSATION.

Bus	t_{CCT}^{0}	t_{CCT}^{com}	Δt_{CCT}
7	223 ms	230 ms	7 ms
8	297 ms	311 ms	14 ms
9	248 ms	256 ms	8 ms
6	377 ms	404 ms	27 ms
5	349 ms	352 ms	3 ms
4	301 ms	310 ms	9 ms

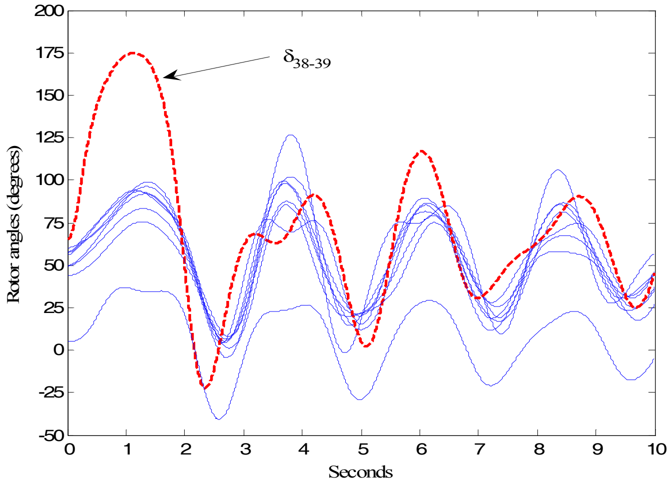

Figure 6. Relative rotor angles.

Finally, the comparison of the *CCT*s for the base case and compensation on line 26-29 is shown in Table IV regarding to faults at all nodes in the weak area, one at the time. It is observed in the last column of this table that in all cases the *CCT* improved when compensation was embedded in the most sensitive transmission line, improving the transient stability margin in the area. The best improvement was obtained when the fault is applied at bus 28, increasing the *CCT* in 20 ms, whereas the *CCT* is marginally improved by 9 ms when the fault is applied at bus 25.

VI. Conclusions

In this paper, a systematic trajectory sensitivity-based approach has been proposed to determine the proper allocation of series-connected controllers in order to improve the transient stability margin of power systems. The approach is completely general and its application does not depend on the kind of series controller to be installed in the system. Guidelines to identify the most suitable location are given according to the relation between sensitivities of relative rotor angle with respect to line susceptances and an index to proximity to instability. Numerical examples on two benchmark power systems are provided and confirm the feasibility as well as the validity of the formulation. The proposed approach is an effective and practical method which could be used for large-scale power systems planning and operation.

Table III. η for each faulted node of the New-England system.

Line Reactance	η for a faulted node				
	Bus 25	Bus 26	Bus 27	Bus 28	Bus 29
B_{26-29}	6.56	4.53	4.37	4.54	4.57
B_{26-28}	13.34	9.13	8.87	9.08	9.13
B_{25-26}	22.27	13.30	12.23	12.79	13.05
B_{28-29}	69.54	49.83	47.23	50.62	50.93
B_{26-27}	58.43	56.51	58.67	54.17	53.49

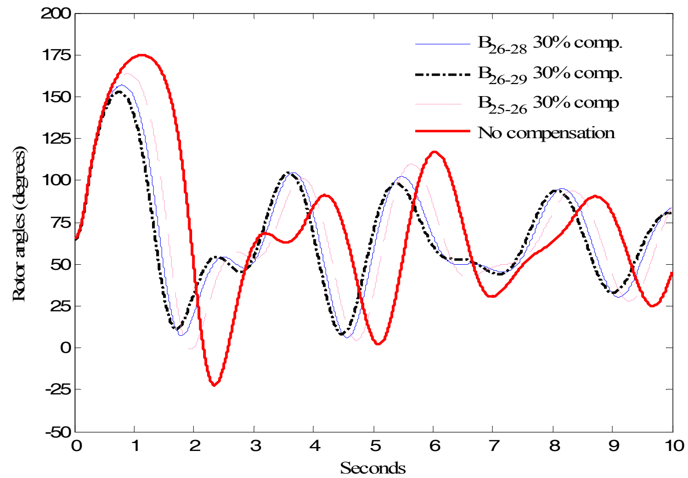

Figure 7. Transient stability improvement.

Table IV. *CCT*s with compensation.

Bus	t^0_{CCT}	t^{com}_{CCT}	Δt_{CCT}
25	300 ms	309 ms	9 ms
26	227 ms	238 ms	11 ms
27	307 ms	323 ms	16 ms
28	230 ms	250 ms	20 ms
29	197 ms	209 ms	12 ms

VII. References

[1] E. Acha, C.R. Fuerte-Esquivel, H. Ambriz-Perez and C. Angeles-Camacho, *FACTS: Modelling and Simulation in Power Networks*, John Wiley & Sons, 2004.

[2] Song Y.H. and Johns A.T. (Editors), *Flexible AC Transmission Systems (FACTS)*, IEE Power and Energy series 30, 1999.

[3] A.Z. Gamm, and I.I. Golub, “Determination of locations for FACTS and energy storage by the singular analysis,” in *Proc. of International Conference on Power System Technology, POWERCON '98*., pp. 411-414.

[4] Y. Mansour, W. Xu, F. Alvarado, and C. Rinzin, “SVC placement using critical modes of voltage stability,” *IEEE Trans. Power Syst.* Vol. 9, pp. 757-762, May 1994.

[5] W.L. Fang, and H.W. Ngan, “Optimising location of unified power flow controllers using the method of augmented Lagrange multipliers,” *IEE Proc.-Gener. Transm. Distrib*, Vol. 146, pp. 428-434, Sep. 1999.

[6] P.Paterni, S. Vitet, M. Bena, and A. Yokoyama, “Optimal location of phase shifters in the French network by genetic algorithm,” *IEEE Trans. Power Syst.* Vol. 14, pp. 37-42, Feb. 1999.

[7] S. Gerbex, R. Cherkaoui, and A.J. Germond, “Optimal location of FACTS devices to enhance power system security,” in *Proc. 2003 IEEE Bologna PowerTech Conf.*, 7 pages.

[8] F.G.M. Lima, F.D. Galiana, I. Kockar, and J. Munoz, “Phase shifter placement in large-scale systems via mixed integer linear programming,” *IEEE Trans. Power Syst.* Vol. 18, pp. 1029-1034, Aug. 2003.

[9] C.A. Cañizares, and Z.T. Faur, “Analysis of SVC and TCSC controllers in voltage collapse”, *IEEE Trans. Power Syst.* Vol. 14, pp. 158-165, Feb. 1999.

[10] S.N. Singh, and A.K. David, “Optimal location of FACTS devices for congestion management,” *Elect. Power Syst. Res.*, Vol. 58, pp. 71-79, Jun. 2001.

[11] N. Martins, and L. Lima, “Determination of suitable location for power systems stabilizers and static VAR compensators for damping electromechanical oscillations in large power systems,” *IEEE Trans. Power Syst.* Vol. 5, No. 4, pp. 1455-1469, Nov. 1990.

[12] H. Okamoto, A. Kurita and Y. Sekine, “A methods for identification of effective locations of variable impedance apparatus on enhancement of steady-state stability in large scale power systems,” *IEEE Trans. Power Syst.* Vol. 10, No. 3, pp. 1401-1407, Aug. 1995.

[13] H.F. Wang, “Selection of robust installing locations and feedback signals of FACTS-based stabilizers in multi-machine power systems,” *IEEE Trans. Power Syst.* Vol. 14, No. 2, pp. 569-574, May. 1999.

[14] R. Sadikovic, G. Andersson and P. Korba, Method for Location of FACTS for Multiple Control Objectives, X SEPOPE, Brasil, May 2006.

[15] N. Magaji and M.W. Mustafa, "Optimal location of FACTS devices for damping oscillations using residue factor," in *Proc 2008 2nd Int. Conf. on Power and Energy*, pp. 1339-1344.

[16] P. Kundur, *Power System Stability and Control*, McGraw Hill, 1994.

[17] M. J. Laufenberg and M. A Pai., "A new approach to dynamic security assessment using trajectory sensitivities," *IEEE Trans. Power Syst.*, Vol. 13, No. 3, pp. 953-958, Aug. 1998.

[18] I.A. Hiskens, M.A. Pai, and T.B. Nguyen, "Bounding uncertainty in power system dynamic simulations," in *Proc 2000 IEEE PES Winter Meeting*, pp. 1533-1537.

[19] I.A. Hiskens, J. Alseddiqui, "Sensitivity, approximation, and uncertainty in power system dynamic simulation", *IEEE Trans. Power Syst.*, Vol. 21, No. 4, pp. 1808-1820, Nov. 2006.

[20] J.J. Sanchez-Gasca, C.J. Bridenbaugh, C.E.J. Bowler, and J.S. Edmonds, "Trajectory sensitivity based identification of synchronous generator and excitation system parameters," *IEEE Trans. Power Syst.*, Vol. 3, No. 4, pp. 1814-1822, Nov. 1988.

[21] S.M. Benchluch and J.H. Chow, "A trajectory sensitivity method for the identification of nonlinear excitation system models," *IEEE Trans. Energy Convers.*, Vol. 8, No. 2, pp. 159-165, June 1993.

[22] I. Hiskens, "Nonlinear dynamic model evaluation from disturbance measurements," *IEEE Trans. Power Syst.* Vol. 16, No. 4, pp. 702-710, Nov. 2001.

[23] T.B. Nguyen and M.A. Pai, "Dynamic security-constrained rescheduling of power systems using trajectory sensitivities," *IEEE Trans. on Power Syst.*, Vol.18, No.2, pp. 848-854, May, 2003

[24] I. Hiskens and M.A. Pai, "Power system application of trajectory sensitivities," in *Proc 2000 IEEE PES Winter Meeting*, pp. 1200-1205.

[25] I. A. Hiskens and M. Akke, "Analysis of the Nordel power grid disturbance of January 1, 1997 using trajectory sensitivities," *IEEE Trans. on Power Syst*., Vol.14, No.3, pp. 987-994, Aug, 1999.

[26] D. Chatterjee and A. Ghosh, "Transient stability assessment of power system containing series and shunt compensators", *IEEE Trans. on Power Syst*., Vol. 22, No. 3, pp.1210-1220, Aug. 2007.

[27] R. Tomovic and M. Vukobratobic, *General Sensitivity Theory*, American Elsevier, New York, 1972.

[28] Khalil H.S., *Nonlinear Systems*, Macmillan, 1992.

[29] I. A. Hiskens and M. A. Pai, "Trajectory sensitivity analysis of hybrid systems," *IEEE Trans. on Circ. and Syst.*-I, Vol. 47, No. 2, pp. 204-220, Feb. 2000.

[30] M. Caracotsios and W.E. Stewart, "Sensitivity analysis of initial value problems with mixed ODEs and algebraic constraints," *Comp. Chem. Engrg.*, Vol. 9, pp. 359-365, 1985.

VIII. Biographies

Enrique A. Zamora-Cardenas received the B.Eng. (Hons.) degree in 1999 from the University of Colima, Colima, México, and the MS degree in 2004 from the Universidad Michoacana de San Nicolás de Hidalgo (UMSNH), Morelia, México, in 2004. He is currently pursuing the PhD degree in UMSNH in the area of dynamic and steady-state analysis of FACTS. He is also an Associate Professor at the Instituto Tecnológico Superior of Irapuato, at Irapuato, Guanajuato, México.

Claudio R. Fuerte-Esquivel (M'91) received the B.Eng. (Hons.) degree from the Instituto Tecnológico de Morelia, Morelia, México, in 1990, the MS degree (*summa cum laude*) from the Instituto Politécnico Nacional, México, in 1993, and the PhD degree from the University of Glasgow, Glasgow, Scotland, U.K., in 1997. Currently, he is an Associate Professor at the Universidad Michoacana de San Nicolás de Hidalgo (UMSNH), Morelia, where his research interests lie in the dynamic and steady-state analyzes of FACTS.